Available online at www.sciencedirect.com

SCIENCE DIRECT®

Journal of Volcanology and Geothermal Research 135 (2004) 75–89

Journal of volcanology and geothermal research

www.elsevier.com/locate/jvolgeores

Thermal infrared remote sensing of volcanic emissions using the moderate resolution imaging spectroradiometer

I.M. Watson[a,*], V.J. Realmuto[b,1], W.I. Rose[a], A.J. Prata[c], G.J.S. Bluth[a], Y. Gu[a], C.E. Bader[a], T. Yu[a]

[a] *Department of Geological and Mining Engineering and Sciences, Michigan Technological University, 1400 Townsend Drive, Houghton, MI 49931-1295, USA*

[b] *Visualization and Scientific Animation, Jet Propulsion Laboratory, 4800 Oak Grove Drive, Pasadena, CA 91109-8099, USA*

[c] *CSIRO Atmospheric Research, PB 1, Aspendale, Victoria, Australia*

Accepted 5 December 2003

Abstract

The volcanological community has a powerful new tool in the spaceborne moderate resolution imaging spectroradiometer (MODIS), which, from its synoptic perspective, provides satellite imagery of every volcano on Earth every 2 days. MODIS has the spectral characteristics to be able to utilise previously developed retrievals that quantify volcanic ash, ice, sulfates and sulfur dioxide using their thermal infrared (8–12 μm) transmission signature. In this paper, we present a detailed description of the methodologies, based within the thermal infrared region, that are being applied to MODIS data. MODIS data for two eruptions, Hekla, Iceland and Cleveland, Alaska are presented to show results from the ice, ash and SO_2 retrieval schemes. We look at current problems with the retrievals used to quantify volcanic emissions, detail recent developments within the field that can be applied to MODIS data, and suggest areas where improvements need to be made in the future.
Published by Elsevier B.V.

Keywords: MODIS; infrared; remote sensing; volcanic emissions

1. Introduction

During an eruption, volcanoes can produce large amounts of gas (H_2O, SO_2, CO_2, HCl, HF, H_2S, etc.) and aerosols (aqueous phase droplets—typically sulfates—ice and silicate ash, suspended in either volcanic gases and/or air), which are studied from several perspectives. These include, but are not limited to: (1) aircraft hazard mitigation-ash can be extremely hazardous to aircraft through ingestion into jet engines (Casadevall, 1994); (2) climatology-ash, and particularly sulfates derived from degassing, can perturb the climate system (Lacis et al., 1992); (3) local environment effects, such as damage to crops and the local population's health (Baxter et al., 1999); and (4) volcanology-gas, liquid and solid phase emissions contain information pertaining to the volcanic system of origin (Rose et al., 2000, 2001).

Following its launch on 18 December 1999, the moderate resolution imaging spectroradiometer

* Corresponding author. Tel.: +1-906-487-2045; fax: +1-906-487-3371.

E-mail address: watson@mtu.edu (I.M. Watson).

[1] Tel.: +1-818-354-1824.

0377-0273/$ - see front matter. Published by Elsevier B.V.
doi:10.1016/j.jvolgeores.2003.12.017

(MODIS) sensor, aboard NASA's Terra platform, has captured images of volcanic eruptions worldwide. MODIS is NASA's flagship sensor system with 36 spectral bands in the visible and infrared (from near to thermal) region of the spectrum (0.4–14.4 μm). Two of its bands operate at a nominal spatial resolution of 250 m at nadir, with five bands at 500 m and the remaining 29 bands, including the thermal infrared bands of interest, at 1000 m. A ±55° field of view from the Terra orbit of 705 km altitude a.s.l. achieves a 2330-km swath and provides global coverage every 1–2 days (http://modis.gsf.nasa.gov).

MODIS has the 'split-window' channels [31,32] at ca. 11 and 12 μm used to observe (Prata, 1989a,b) and quantify silicate ash (Wen and Rose, 1994) and ice (Rose et al., 1995). It also has a channel centred at 8.65 μm [29] that can be used (with the 'split-window' channels) to quantify SO_2 burdens (Realmuto et al., 1994, 1997; Realmuto and Worden, 2000). We can also incorporate recent modifications including an atmospheric correction (Yu et al., 2002) and multi-band sulfate retrieval, using all channels, including the 9.7-μm channel [30] (Yu and Rose, 2001), and a new SO_2 algorithm using the 7.3-μm channel [28] (Prata et al., 2003, in review). All these algorithms use the spectral attenuation of infrared terrestrial radiation, between 7 and 13 μm, by volcanic species to quantify emissions during and after a volcanic event.

Each of the algorithms was designed using a particular combination of bands from differing satellites and airborne sensors (Table 1). We have taken the retrievals, previously developed for other sensors such as the spaceborne Advanced Very High Resolution Radiometer (AVHRR) and Geostationary Operational Environmental Satellite (GOES) or the airborne Thermal Infrared Mapping Spectrometer (TIMS), and applied them, with some modifications to MODIS data. Some of the retrievals, such as those based about TIMS, were designed specifically with MODIS in mind (Realmuto, 2000). Some specific examples of retrievals using MODIS are in Bluth et al. (in prep.)—the Nyamuragira eruption (2001) and Rose et al. (2003).

Table 1
Applications of MODIS TIR channels

Channel number	Wavelength (μm)	Applications	Resolution (km)
28	7.175–7.475	H_2O, SO_2	1
29	8.400–8.700	SO_2, SO_4^{2-}	1
30	9.580–9.880	SO_4^{2-}, O_3	1
31	10.780–11.280	ice, ash, SO_4^{2-}	1
32	11.770–12.270	ice, ash, SO_4^{2-}	1

One significant improvement in using MODIS data to observe volcanic emissions is that we can now measure co-erupted species from the same image. This facilitates observation of the fates of volcanic species, particularly conversion rates of SO_2 to SO_4^{2-} as both products can be mapped within the same image. It also allows us to observe separation of species, for example through either early release of SO_2 before a paroxysm or gas-ash separation of the drifting cloud through wind sheer effects.

The aims of this paper are to provide an overview of volcanic emission detection using MODIS (and other new thermal infrared sensors) and a detailed, coherent description of the methodologies currently being employed and tested. There are many potential improvements that can be made to the retrievals developed for MODIS, particularly in the understanding of how volcanic species interact with each other through time, and the complex spectral effects of other volcanic species and the atmosphere on remote sensing techniques. It is hoped that this paper will illuminate these problems and suggest potential solutions, as well as bring the issues to the attention of a wider audience.

2. Nomenclature

We attempt to standardize the nomenclature of previous work into a single scheme. Where significant differences occur they are explained. We have consistently used the subscript c for volcanic cloud (and/or plume), λ for spectral terms, a for atmospheric and g for ground parameters.

d	cloud thickness
h	cloud height
L_d	downwelling radiance (ambient, sky radiance at the ground)
L_s	at-sensor radiance
L_u	upwelling radiance (ambient, sky radiance at the sensor)

L_{ucb} upwelling radiance at the cloud base (I_s in Yu and Rose, 2000)
r_c reflectivity of the cloud
r_g reflectivity of the ground
r_e effective radius
t_a transmission of the atmosphere
t_c transmission of the cloud
T_{cb} cloud base temperature
T_{ct} cloud top temperature
T_g ground temperature
ΔT brightness temperature difference (BTD) of channels at approx. 11 and 12 μm
Q_{abs} absorption efficiency factor derived from Mie theory
N particle number density
B Planck function
ε_c emissivity of the cloud
ε_g emissivity of the ground
λ wavelength
τ_a optical depth of the atmosphere
τ_c optical depth of the cloud
[28] MODIS channels are contained within square parenthesis

3. Theoretical overview

3.1. Silicate ash

Prata (1989a,b) first proposed using the thermal infrared transmissive properties of volcanic ash clouds to track, by discriminating volcanic clouds from background, within satellite images. The transmission spectrum of volcanic ash clouds is strongly wavelength dependent and has a broad absorption-related feature between 8 and 12 μm (Fig. 1B), typically centred near 9 μm but varying according to composition. A two-channel difference model was proposed based upon the absorption feature and the location of the 11- and 12-μm channels [4,5] of the AVHRR, analogous to channels [31,32] of MODIS. It was shown that the at-sensor radiance can be approximated as:

$$L_s \approx e^{-\tau c} B(T_g) + (1 - e^{-\tau c}) B(T_c) \quad (1)$$

and that the difference between the at-sensor radiances, and thus Planck brightness temperatures, observed in two channels located at ca. 11 and 12 μm (i and j in the

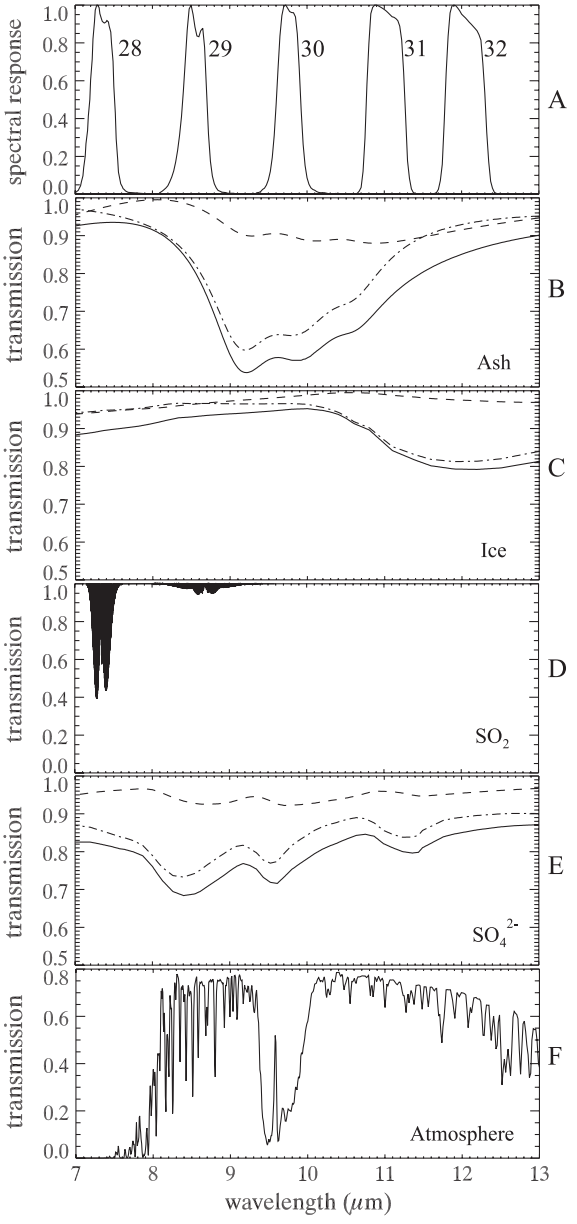

Fig. 1. (A) MODIS spectral response functions for channels [28–32]; (B) total (solid line), absorptive (dotted and dashed line) and scattering (dashed line) transmission spectra of andesitic ash, $r_e = 3.0$, $N = 5 \times 10^6$ particles/cm^2; (C) total (solid line), absorptive (dotted and dashed line) and scattering (dashed line) transmission spectra of ice, $r_e = 3.0$, $N = 5 \times 10^6$ particles/cm^2; (D) transmission spectrum of SO_2 showing relative strengths of 7.3 and 8.6 μm absorption features (E) total (solid line), absorptive (dotted and dashed line) and scattering (dashed line) transmission spectra of 75% sulfate, 25% water droplets, $r_e = 3.0$, $N = 5 \times 10^6$ particles/cm^2; (F) transmission spectrum of a dry, northern latitude summer atmosphere.

original paper), respectively, are negative ($-\Delta T$) if the ash cloud is partially transparent and that $T_g > T_c$. This is due to the fact that ash attenuates, mostly through absorption, more strongly at 11 than at 12 μm (Fig. 1B). Discrimination from non-volcanic (background) pixels is made possible by the fact that water in any phase will have a positive effect on the brightness temperature difference (BTD or ΔT). As an aside, it is worth noting that, as water vapour has an effect countering that of volcanic ash, it is possible to mask the negative BTD signal from ash with water vapour, liquid droplets and ice (see Section 6).

Wen and Rose (1994) built on early work (Prata, 1989a,b) and developed a retrieval scheme that quantifies the effective scattering radius (the radius associated with the average surface area) and optical depth (and hence the mass) of a volcanic ash cloud. Starting with an analogue of Eq. (1), Wen and Rose (1994) defined the at-sensor radiance as:

$$L_s = t_c B(T_g) + \varepsilon_c B(T_c) \quad (2)$$

as

$$t_c = e^{-\tau c} \text{ and } \varepsilon_c \approx 1 - e^{-\tau c} \quad (3a \text{ and } b)$$

However, an extra consideration, the cloud reflectivity, was added to the equation as:

$$\varepsilon_c = 1 - t_c - r_c \quad (4)$$

Rearrangement and substitution of Eq. (4) into Eq. (2) yields Eq. (2) from Wen and Rose (1994):

$$L_s = (1 - r_c(r_e, \tau_c))B(T_c) + t_c(r_e, \tau_c)(B(T_s) - B(T_c))) \quad (5)$$

Given a theoretical radiance pair ($L_s i$ and $L_s j$), calculated by defining r_e and τ_c, the corresponding brightness temperatures can be calculated using the Planck function. This allows a theoretical look-up-table (LUT) to be generated for sets of variations of both r_e and τ_c a function of brightness temperature, and hence a value of r_e and τ_c to be retrieved for any given brightness temperature pair.

3.2. Ice

The methodology for the ice retrieval (Rose et al., 1995) is very similar to that of ash, except that ice's $+\Delta T$ signal is used to locate and quantify the volcanogenic ice clouds (Fig. 1C). In principle, it is assumed that the ice signal from a volcanogenic source will be more positive than the surrounding atmosphere. Again, this is due to the position of an absorption feature, this time centred at 12 μm. Hence, the transmission of infrared radiation, and thus the brightness temperature, is lower at 12 μm compared to 11 μm, making the brightness temperature difference signal for ice positive. The mass retrieval (Wen and Rose, 1994) was straightforwardly adapted simply using ice's refractive index instead of ash's.

3.3. SO_2

The SO_2 retrieval is also based on the wavelength dependence of absorption features (Fig. 1D). Again, the theoretical basis for the retrieval began with another slightly altered, general expression of the at-sensor radiance, from Realmuto et al. (1994):

$$L_s = \{\varepsilon_g B(T_g) + (1 - \varepsilon_g)L_d\} t_a + L_u \quad (6)$$

Here, two additional (atmospheric) terms (L_u and L_d) are included that describe the column-integrated ambient (sky) radiance at the sensor and the ground, respectively. The downwelling term is multiplied by the reflectivity of the ground (the transmissivity of the ground is defined as 0 so $r_g = 1 - \varepsilon_g$) and added to the emission term to yield the ground-leaving radiance (defined within the curly brackets). The spectral emissivity of the ground is calculated using spectral normalization (Realmuto, 1990), where the maximum ground emissivity is set by the user. The ground-leaving radiance is then multiplied by the transmission of the atmosphere and the upwelling radiance is added. Eq. (6) is solved for T_g for the channels outside the SO_2 absorption feature to yield the 'true' ground temperature. The upwelling and downwelling radiances and the transmission of a user-defined atmosphere are derived using the MODTRAN radiative transfer code (Berk et al., 1989). Then Eq. (6) is solved for T_g for the channel(s) inside the absorption feature yielding the 'apparent' ground temperature. The difference between the true and perceived ground radiance is a function of the SO_2 burden (given the absence of other attenuators).

3.4. Sulfates

Extending the work of Wen and Rose (1994) permits investigation of co-emitted sulfate and ash (Yu and Rose, 2001). Rearranging Eq. (2), and using the Beer-Lambert law, Yu and Rose (2001) constructed a general expression for the at-sensor radiance using a new term—the upwelling radiance at the cloud base (L_{ucb}). They defined the at-sensor radiance as follows (after some nomenclature change and substituting the expressions (3a) and (3b)):

$$L_s = \tau_c L_{ucb} + \varepsilon_c B(T_c) \quad (7)$$

where L_{ucb} is similar to the ground leaving radiance L_g in Eq. (2) but can incorporate the downwelling term from Eq. (6). Again, MODTRAN is used to derive L_{ucb}. Eq. (7) is solved with respect to τ_c for each wavelength and then related to the scattering properties of the two species through the equation:

$$\tau = N_1 \pi r_{e1}^2 Q_{abs1} d + N_2 \pi r_{e2}^2 Q_{abs_2} d \quad (8)$$

where the subscripts 1 and 2 relate to the separate species. A LUT is generated using 2300 pairs of radii and the non-negative best fit between the LUT and the optical depths from Eq. (7) are determined to be the effective radii of the ash and sulfate particles. SO_4^{2-} has a more complex transmission spectrum (Fig. 1E) and hence requires more pieces of information to adequately constrain the particle size distribution, especially given the fact that the concentration of aqueous SO_4^{2-} can vary. The refractive index of SO_4^{2-} is sensitive to its concentration within the droplet, and the sulfate's transmissive properties are also very sensitive to changes in size distribution.

4. Recent developments

4.1. Atmospheric correction of ash retrievals

Recent literature has highlighted the important role the atmosphere, in particular atmospheric water vapour, plays in infrared retrievals of volcanic emissions (Simpson et al., 2000; Realmuto and Worden, 2000; Prata et al., 2001). Yu et al. (2002) have developed a simple, empirical correction for atmospheric water vapour, which was analysed using a model based around MODTRAN, for the Wen and Rose (1994) ash retrieval. The correction uses a 'cutoff' based upon brightness temperatures and brightness temperature differences, rather than solely brightness temperature differences. This allows for more complex definitions of how pixels are classified and has the effect of correctly classifying most 'non-volcanic' pixels in the image. The other criteria for volcanic pixels is their contiguity—if pixels are classified as volcanic using the cutoff method, but are separate from the core of the cloud (defined as BTD < 0) then they are assigned non-volcanic.

It was found that for dry, high latitude clouds water vapour interference tended only to mask the fringes of the volcanic cloud (Yu et al., 2002) and that, whilst the cloud area increased significantly (ca. 50%), the effective radius, mean optical depth and, most importantly the fine ash mass, were relatively unaffected (< 20%). The effects of tropical water vapour upon the ash retrieval were, as expected, more significant. The cloud area increased by a factor of 5, and the effective radius halved as more fine ash, at the fringes of the cloud, was observed. Again the total tonnage was relatively unaffected, suggesting that the core of the cloud, observable in almost all cases, contains the bulk of the ash mass.

4.2. SO_2 mapping water vapour correction

It is vital to understand the effects of atmospheric water vapour upon retrievals based in the thermal IR (Realmuto, 2001). In the first generation of SO_2 mapping algorithms, a atmospheric profile was used to calculate the contribution of atmospheric water vapour to the at-satellite radiance (through t_a, L_u and L_d in Eq. (6)). These parameters were subsequently applied to

Table 2
Previously developed algorithms applied to MODIS infrared data

Species	Sensor	Sensor channels	MODIS channels	References
Ash	AVHRR	4, 5	31, 32	Prata (1989a,b)
Ash	AVHRR, GOES	4, 5	31, 32	Wen and Rose (1994)
Ice	AVHRR, GOES	4, 5	32, 32	Rose et al. (1995)
SO_2	TIMS, MODIS	1–6	29–32	Realmuto et al. (1994, 1997, 2000)
SO_4^{2-}	HIRS/2	5–10	30, 31–34	Yu and Rose (2001)

the entire image. It was subsequently realised that water vapour is highly variable, even at the spatial scales of the imagery (Realmuto and Watson, 2001) and that, given the perceived ground temperature is wavelength dependent and the 'true' ground temperature is wavelength independent, following a correction for emis-

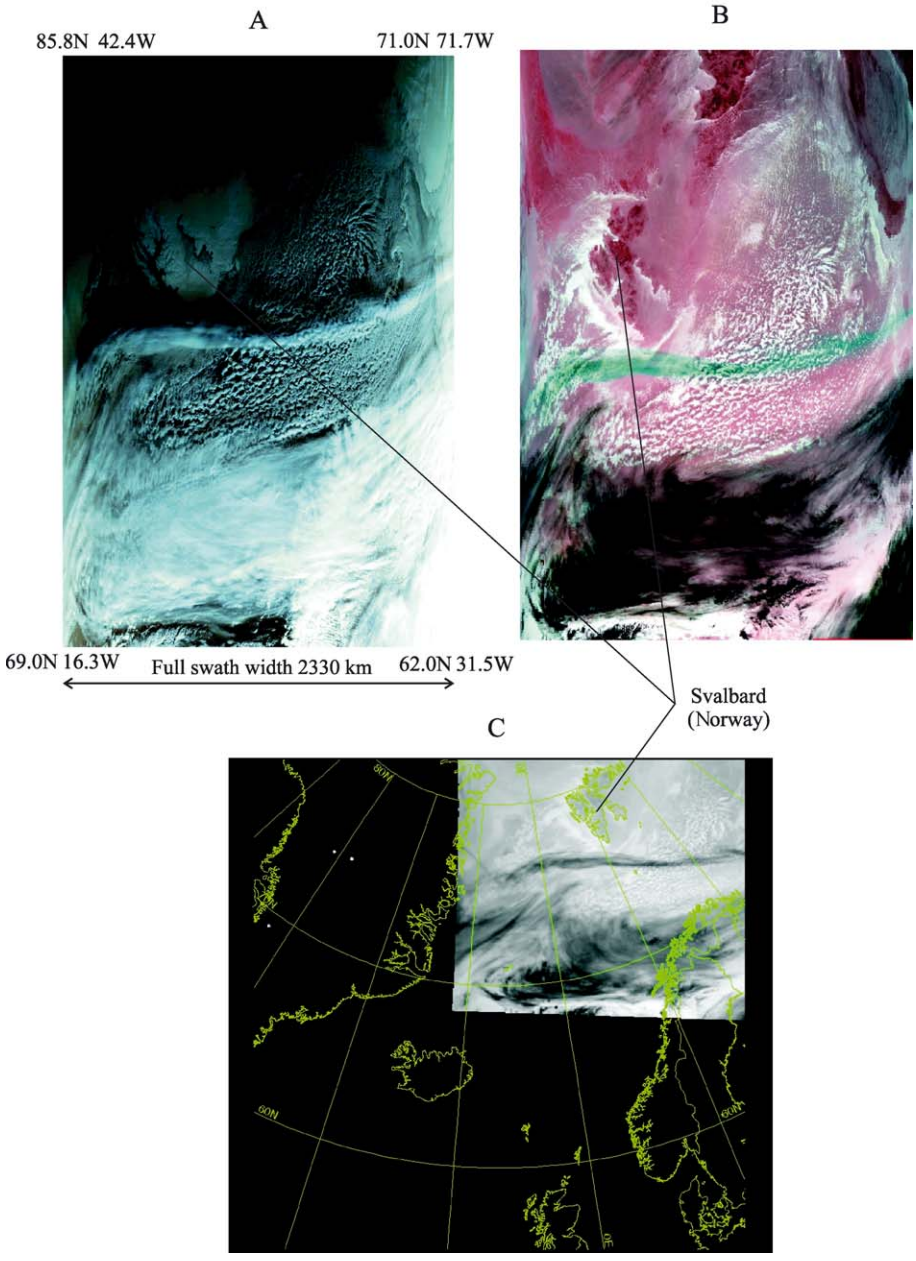

Fig. 2. (A) Channel [1], 0.62–0.67 μm, MODIS image of the Hekla eruption cloud, acquired at 1115 UT on 28 February 2000 at 250-m spatial resolution; (B) the same image as (A) using red–green–blue [28,31,32] composite at 1-km resolution; (C) the same image georeferenced—single channel [28]—showing location of SO_2 cloud relative to geographic boundaries.

sivity, spectral variations in the ground temperature can be attributed to atmospheric absorption and emmision. Thus, in principle, it is possible to use MODTRAN to calculate the amount of water vapour needed to 'flatten' the perceived ground temperature by iterating through water vapour concentrations until the flattest spectrum is achieved. As each pixel has a specific perceived ground temperature spectrum, it is possible to map water vapour on a pixel-wise basis. Early results suggest that, while the model requires additional runs of MODTRAN per pixel, it is possible to map water vapour (and potentially ozone) using this method, and that the SO_2 retrieval is more robust.

4.3. Forward modelling sensitivity analysis

We have written an aerosol forward model, based around Mie scattering code, and embedded it in a MODTRAN-based atmospheric model (Watson et al., submitted for publication). The model allows us to perform a sensitivity analysis of the ash and sulfate retrieval schemes, and more importantly, to quantify the effects of atmospheric water vapour on the various retrievals. The model requires the definition of the aerosol, the atmosphere and the primary source of the infrared radiation, usually the ground. The aerosol is defined by a particle size distribution, a wavelength dependent refractive index and a total burden (in either units of number or mass). The atmosphere is defined by pressure, temperature and relative humidity profiles typically acquired by radiosonde. The ground is defined in terms of its temperature and spectral emissivity.

The model produces spectra of transmission of both the aerosol and the total system and at-satellite radiance (or brightness temperature). Water vapour concentrations can be varied to test the sensitivity of the 'split-window' retrieval. Preliminary results suggest that the tropospheric water vapour burdens are more than sufficient to mask all but the strongest negative signal associated with ash. The water vapour above Soufriere

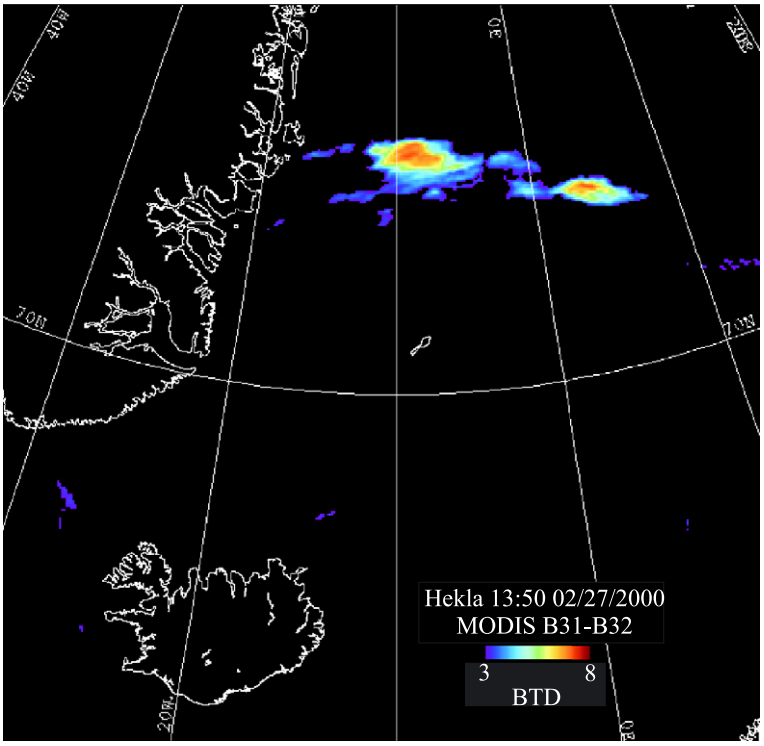

Fig. 3. Brightness temperature difference map from an image of the Hekla volcanic cloud acquired at 1350UT on 27 February 2000 showing positive BTD values indicative of ice. The total mass of the ice cloud was ca. 200 kt.

Hills volcano has a positive effect of as much as 3.5 K upon the brightness temperature difference signal (Watson et al., submitted for publication).

4.4. 7.3 μm channel SO_2 quantification

SO_2 has a second, stronger absorption feature centred at 7.34 μm (Fig. 1D), which can also be used to quantify volcanic SO_2, using MODIS (Prata et al., in review) and TIROS Operational Vertical Sounder (TOVS) (Prata et al., 2003) data. A complete description of the retrieval schemes for both sensors is given in the above papers. Briefly, as the atmosphere is opaque at this wavelength (Fig. 1F), due to water absorption, the retrieval uses the fact that the water vapour itself emits at that wavelength, and that SO_2 above the water vapour, contained mostly (95%) in the bottom 6 km of the atmosphere, will absorb upwelling radiance from the water vapour. The method has its limitations as the SO_2 must be well above the penetration depth (ca. 3 km) of the vertical sounding 7.3-μm channel [28] of MODIS. However, the method also has distinct spectral advantages as, unlike the 8–12-μm channels [29–32], the shorter IR channels are not strongly affected by the presence of either silicate ash or sulfate aerosol. The only species that will really interfere with the 7.3-μm channel is ice, as its transmission reduces below 8.0 μm (Table 2).

5. Example results

We have chosen two quite different eruption clouds, early in the MODIS data archive, to evaluate the current status of the current suite of IR retrieval schemes. These eruptions are those of Hekla volcano, Iceland on 26–28 February 2000 and Cleveland volcano, Alaska on 19–22 February 2001. The cloud produced by Hekla is likely to be relatively poor in fine ash (Rose et al., 2003) in contrast with Cleveland's ash-laden cloud. The presence (or absence) of solid-phase species has significant effects on the different SO_2 retrievals.

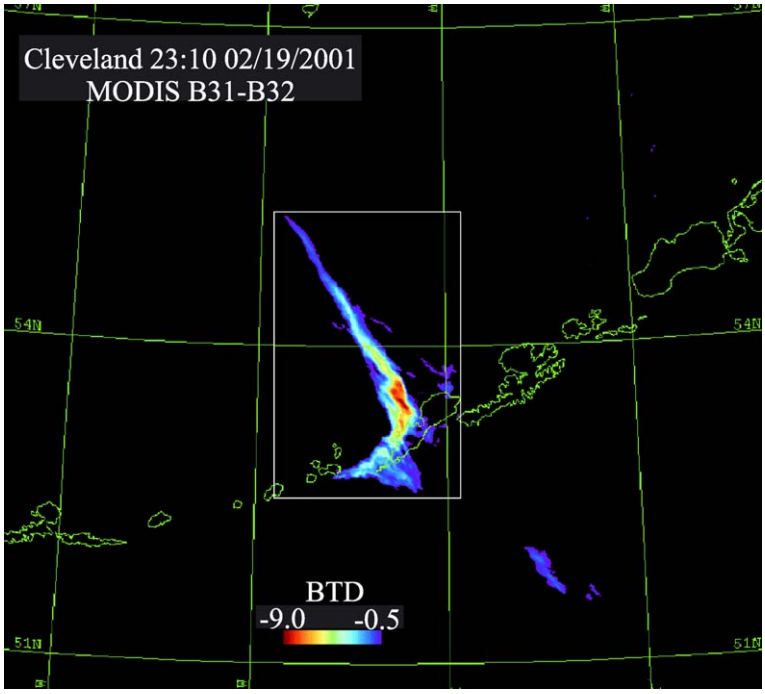

Fig. 4. Brightness temperature difference map from an image of the Cleveland volcanic cloud acquired at 2310 UT on 19 February 2001 showing negative BTD values indicative of ash. The total mass of the ash cloud was ca. 20 kt.

5.1. Hekla Volcano, Iceland (63.9N, 19.7W)

The Hekla volcanic system, located in southern Iceland near the southern end of the east rift zone, is comprised of a central shield-like vent and a series of basaltic fissures and is one of Iceland's most active volcanoes. Its latest eruption began on 26 February 2000 at 1819 UT as a 6–7 km fissure opened producing an eruption column that reached initial heights of >12 km (Rose et al., 2003). The plume generated was observed to be paler than most ash-rich eruption columns suggesting a higher water content. This assumption was borne out by satellite imagery that indicated the presence of significant amounts of ice in the drifting cloud (Rose et al., 2003).

The Hekla volcanic cloud can be seen quite clearly in the raw level 1b MODIS visible radiance data (Fig. 2A) and in the infrared channels (Fig. 2B) from an image acquired at 1115 UT on 28 February 2000. Fig. 2B is a red–green–blue (rgb) composite of channels [28,31,32]–7.3, 11 and 12 μm, respectively from the same image. The cloud is highlighted as channel [28] is highly sensitive to SO_2 and the longer wavelength channels are not. The cloud and its shadow can also be clearly seen in the visible image (2A) re-emphasising the importance of using channels outside the thermal infrared to track volcanic clouds under certain circumstances. The cloud height can be determined from this image, using shadow clinometry, and is approximately 10 ± 2 km. Fig. 2C is a geolocated map of channel [28]–7.3 μm, showing the position of the drifting SO_2 cloud.

Fig. 3 highlights the effect of ice on the brightness temperature difference images derived from MODIS data. The volcanic cloud can be discriminated from the background using the criterion that, specific to this image only, the ice-laden volcanic cloud has a BTD of >3 K. This image, actually earlier than that in Fig. 2, shows the drifting cloud detached from the source. The relatively high cutoff

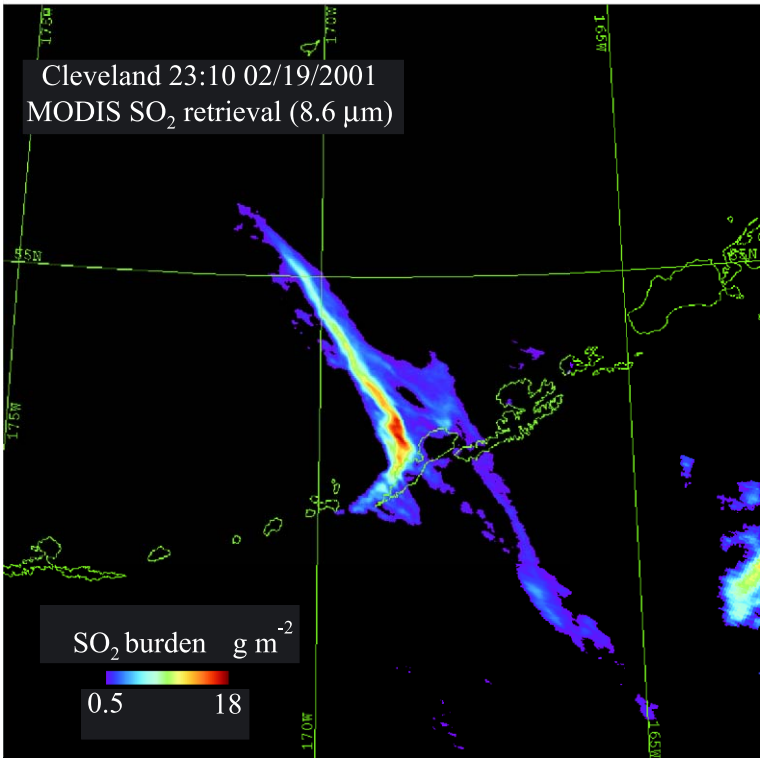

Fig. 5. SO_2 map derived from a MODIS image of the Cleveland volcanic cloud, using the 8.6-μm method, acquired at 2310 UT on 19 February 2001. The total mass of the SO_2 cloud was ca. 60 kt.

(3 K) of the image is required to remove a potentially ice-rich storm system from the image, and therefore the cloud shown is likely to be only the ice-rich, more concentrated core of the cloud. The total mass of the cloud, assuming that it is solely comprised of ice, is calculated to be ca. 200 kt using the Wen and Rose (1994) method.

The SO_2 tonnages derived from the Total Ozone Mapping Spectrometer (TOMS) are in relatively good agreement with the IR retrievals (Rose et al., 2003). TOMS is a series of ultraviolet (UV) spectrometers with an at-nadir footprint of 25–62 km that has observed over 200 eruptive events since the first sensor's launch in 1978 (Carn et al., 2003). TOMS retrievals produced a total cloud mass of SO_2 of 60 kt, compared to 200 kt for the 7.3-μm retrieval and 130 kt for the 8.6-μm retrieval. The 'underestimate' of TOMS in this case is likely to be due to parts of the cloud being too far North for TOMS to observe. The difference between the two IR methods might be explained by the presence of ice, causing an overestimate in the 7.3-μm scheme. The positive BTDs associated with ice diminish and the correlation between the two IR-derived tonnages improves as the cloud ages, suggesting a removal of ice during transport (Rose et al., 2003).

5.2. Cleveland volcano, Alaska (52.5N, 167.6W)

Mt. Cleveland is a stratovolcano located on the western side of Chuginadak Island and is one of the most active volcanoes in the Aleutian island arc. It erupted explosively on 19 February 2001 and generated an ash-rich eruption cloud that was tracked for 3 days using satellite data (Dean et al., 2002). Figs. 4–6 are derived from a MODIS image from early in the cloud's evolution, approximately nine hours after the start of the eruption (1400 UT). Due to the remoteness of the volcano, the eruption was monitored by the Alaska Volcano Observatory (AVO) using mostly satellite imagery.

The volcanic cloud's characteristic ash signal (negative BTD) can be seen in Fig. 4, derived from a MODIS image acquired at 2310 UT on 19 February 2001. The core of the cloud has the strongest

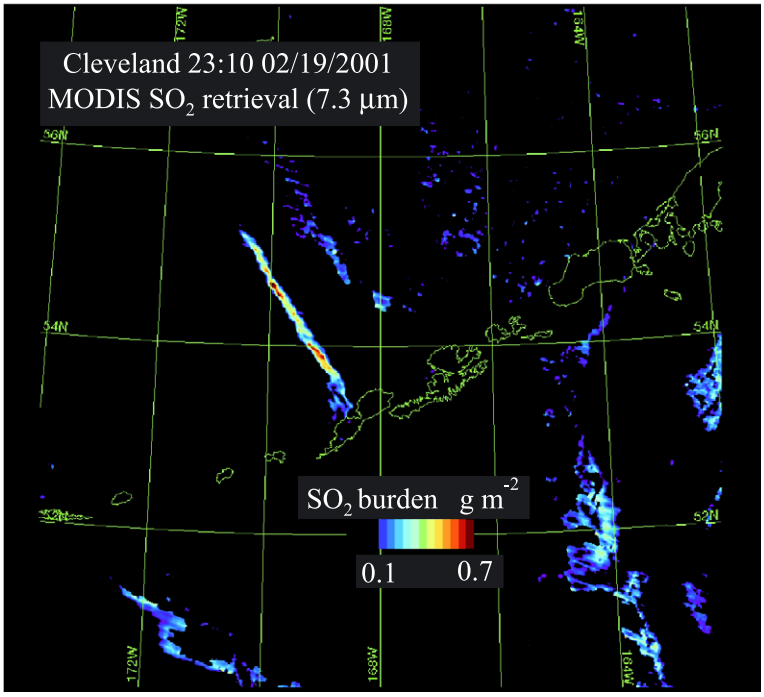

Fig. 6. SO_2 map derived from a MODIS image of the Cleveland volcanic cloud, using the 7.3-μm method, acquired at 2310 UT on 19 February 2001. The total mass of the SO_2 cloud was ca. 5 kt.

negative BTD signal, a ubiquitous feature of 'split-window' imagery of volcanic clouds. The total mass of the ash in the cloud is calculated, using Wen and Rose (1994), to be ca 20 kt. Fig. 5 shows the location of co-erupted SO_2 during the eruption. The high latitude of the cloud suggests that the interference of water vapour upon the ash retrieval should be minimal.

SO_2 cloud burdens were calculated using the 8.6-μm retrieval (Realmuto, 2000) and used to derive a total cloud tonnage for the 19 February image. The ash and the SO_2 appear to be well correlated spatially suggesting little gas-ash separation at this time. This may also be because the 8.6-μm retrieval is ill-equipped to deal with the presence of ash in the cloud, and may be assuming that attenuation of terrestrial radiation by ash is actually caused by SO_2, leading to an overestimate of the burden. The algorithm was specifically designed to observe passively degassed SO_2 with little or no ash content and additional work is required to enable both the SO_2 and ash algorithms perform better when both species are present in significant amounts.

The total mass of the SO_2 cloud derived using the 8.6-μm algorithm is approximately 60 kt. This seems like an overestimate compared to TOMS (15 kt) and the 7.3-μm algorithm (5 kt). 60 kt is likely to be an overestimate due to the presence of ash, whereas 5 kt is likely to be an underestimate due to the eruption cloud's height near vent. The 7.3-μm retrieval is extremely sensitive to cloud height, relative to the altitude of water vapour contained in the atmosphere. The eruption cloud from Cleveland seen in the MODIS image is still attached to the vent, where it is at a lower altitude than the northern-most tip of the vent (Fig. 6). As proximity to the cloud increases the 7.3-μm retrieval can be seen to break down, as the cloud becomes beneath the altitude limit of the sounding channel.

TOMS also captured an image of the Cleveland eruption on 19 February 2001, just an hour before

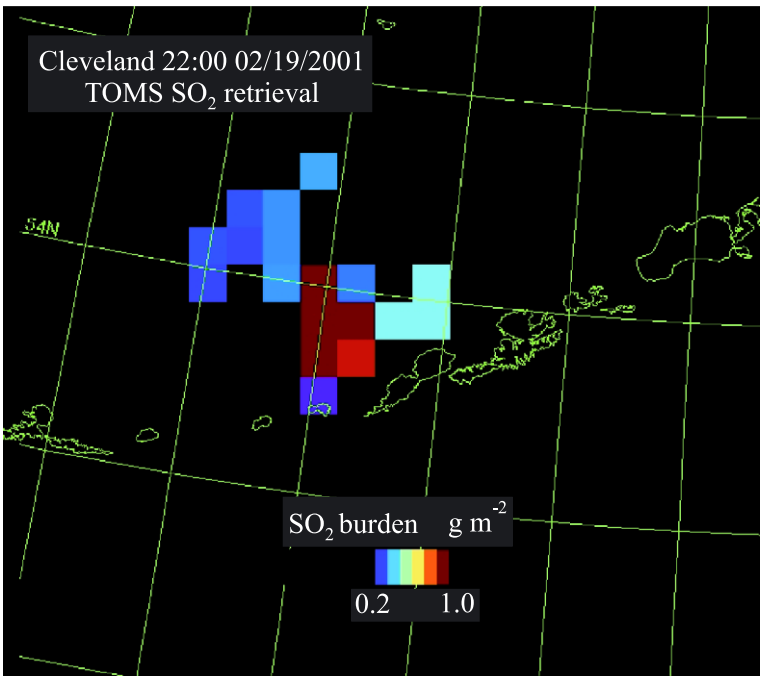

Fig. 7. SO_2 map derived from a TOMS image of the Cleveland volcanic cloud acquired at 2200 UT on 19 February 2001. The total mass of the SO_2 cloud was ca. 20 kt.

the MODIS image. Although TOMS spatial resolution is significantly larger than that of MODIS (one TOMS pixel (at-nadir) contains about 1500 MODIS pixels (near-nadir)) the respective SO_2 maps (Figs. 5–7) are in general agreement. All three SO_2 images show a SW–NE-trending SO_2 cloud observed in the ash retrieval (Fig. 4). Analysis of the TOMS image yields an intermediate cloud tonnage of 20 kt. Of the three tonnages the TOMS tonnage is likely to be the closest to a 'real' SO_2 value, given the complicating factors of high ash content (for the 8.6-μm calculation) and low altitude (for the 7.3-μm calculation). It must again be emphasized that the 8.6-μm algorithm was designed to look at passively degassed SO_2 and that the 7.3-μm algorithm was designed to look at higher, climatologically significant SO_2 emissions.

6. Discussion

6.1. Algorithm limitations

It is clear that, while significant progress has been made in the field of remote sensing of volcanic emissions, much still needs to be done. The reliability of assumptions made about the lack of importance of the atmosphere, specifically to the ash retrieval, is a function of the dryness of the atmosphere. Most of the species we are trying to measure interfere spectrally with each other. None of the five MODIS wavelengths in the 7–13-μm range can be used solely to observe a single species—a direct result of the broadness of the absorption features of the non-gas phase species (ash, ice and sulfate)—unless only that species is present.

We also know very little about the fates of volcanic species in the atmosphere (Oppenheimer et al., 1998)—their reaction rates, deposition rates and their potential for indirect climate forcing through cloud nucleation. Species interaction also confounds our remote sensing algorithms—a commonly used example is the presence of ash in the Hekla eruption cloud (Rose et al., 2003). Course ash was observed to fall out during the early stages of the eruption, and after several hours the eruption cloud had a positive BTD—indicative of the presence of large amounts of ice. Unfortunately this generates an ambiguity; was the ash removed by deposition or simply coated in ice, hiding it spectrally?

6.2. Laboratory studies

Current ash retrievals are based on refractive index (optical constant) measurements taken nearly 30 years ago (Pollack et al., 1973). These measurements, limited to only a handful of volcanic glasses, highlight the paucity of lab-based measurements of volcanic ash. There is a great need for these measurements to be expanded to include the numerous different ash samples collected worldwide. In contrast ice and sulfates are extremely well defined, due to their existence outside volcanism. However, nothing is known about the spectral effects of combinations of these species. For example, how thick does a coating of ice around an ash particle have to be to mask the ash's spectral signature? If the ice does not coat the ash, but remains within the cloud, how much ice is then required to mask the signal? These questions can be answered through laboratory experiments, ground truthing and modelling.

6.3. Ground truthing

One of the most important issues in studying volcanic emissions, particularly ash, is that there is a need for direct, in-plume sampling in order to validate satellite algorithms. Direct sampling is necessary as ash fallout deposits are almost never a reasonable description of the bulk properties of the cloud, as through gravitational settling, only the courser ash particles are deposited; it is the finer ash that typically forms the drifting clouds that are the aircraft hazard. There are two similar methodologies currently under development, both of which involve unmanned airborne vehicles: (1) impactors and filter technology mounted upon remote controlled aircraft (Pieri, pers. comm.); and (2) lightweight kite-borne filter systems designed to capture samples suitable for SEM analysis (Fischer, pers. comm.). Implementation of these techniques during satellite overpasses will vastly improve our understanding of the accuracy of our retrievals, given problems of scaling what are effectively point source data to holistic satellite imagery, and limitations of range and altitude, can be overcome.

Table 3
Applications of different SO_2 retrievals

Retrieval	Application	Disadvantages
TOMS (0.3–0.36 μm)	Large-scale eruptions	Spatial resolution
MODIS (7.34 μm)	Mid-scale eruptions	High altitude required, some ice interference
MODIS (8.6 μm)	Mid-scale to passive degassing	Strong ash and sulfate interference

6.4. SO_2 retrievals at different scales

MODIS data offer a spectrally independent, higher resolution addition to widely used TOMS data. MODIS data provide an excellent complement to TOMS data in that MODIS is able to observe the smaller eruptions whilst TOMS is able, through an advantageous spectral setting (0.30–0.32 μm), to quantify larger emissions in what can be considered a solely scattering atmosphere. TOMS data have not really been subjected to such a rigorous investigation of errors; some of the methodologies shortcomings have been discussed (Krueger et al., 1995). With the impending addition of the 7.3-μm MODIS retrieval (Prata et al., in review), there now exist three distinct methodologies with applications of differing scales from passive degassing (Watson et al., in preparation) to Pinatubo-sized events (Table 3). We have already acquired data that will allow us to compare TOMS and MODIS retrievals and hope to present results of comparisons shortly.

7. Conclusions

MODIS has a suite of thermal infrared channels whose analogues, on AVHRR, GOES and TIMS sensors, have already been used to observe and quantify volcanic clouds containing SO_2, SO_4^{2-}, ice and silicate ash. MODIS data have the huge advantage of containing information about all of the above species, given their presence, within a single image. The difficulties arise from attempting to disentangle the spectral contributions of the different species, and their physical and chemical interactions within the plume. The more pieces of information, i.e. in this case the number of channels of the radiometers, the better constrained the inversion of the data.

We have begun applying algorithms to MODIS data in order to retrieve information pertaining to volcanic eruptions. The first significant eruption MODIS observed was that of Hekla Volcano, Iceland in early 2000. The eruption was somewhat anomalous in that the volcanic cloud appeared to contain a significant proportion of ice, masking the typical negative BTD signal associated with ash-rich volcanic clouds. The total mass of ice in the cloud was calculated to be on the order of 200 kt. The eruption of Cleveland volcano, Alaska, provided a more 'typical' volcanic cloud, characterised by a strong negative BTD signal. We calculated both ash and SO_2 masses for the Cleveland cloud. The eruption appears to have produced approximately 20 kt of fine both fine ash and SO_2.

Our algorithms can be improved through updated laboratory measurements, ground truthing and sensitivity analyses using forward models. We now have more TIR channels, and therefore can use several pieces of information in our inversions, providing a more robust analysis (Ackerman, 1997); band combinations are being tested to facilitate improved retrievals. Specific problems require addressing in the near future; for example water vapour masks the negative BTD signal of ash due to a water absorption feature at >12.0 μm. This is especially a problem in the tropics where the water vapour effect can overwhelm the ash signal to the extent that the MODIS image no longer contains any negative pixels. It is possible to calculate, and thus remove, the effects of water vapour through modelling. Ground truthing is an important step towards determining the accuracy of satellite-based retrievals.

Acknowledgements

Funding for this work was provided by NSF (Petrology and Geochemistry Grant 9725682), NASA (SENH Grant NAG5-11062 and JPL contract #1212354) and the Michigan Space Grant Consortium. Clive Oppenheimer and Dave Schneider greatly improved the manuscript through thorough and thoughtful review.

References

Ackerman, S.A., 1997. Remote sensing aerosols using satellite infrared observations. Journal of Geophysical Research 102 (D14), 17069–17079.

Baxter, P.J., Bonadonna, C., Dupree, R., Hards, V.L., Kohn, S.C., Murphy, M.D., Nichols, A., Nicholson, R.A., Norton, G., Searl, A., Sparks, R.S.J., Vickers, B.P., 1999. Cristobalite in volcanic ash of the Soufriere Hills Volcano, Montserrat, British West Indies. Science 283 (5405), 1142–1145.

Berk, A., Berstein, S., Robertson, D.C., 1989. MODTRAN: a medium resolution model LOWTRAN-7, Tech. Rep., GL-TR-89-0122, Geophys. Lab., Hanscom AFB, MA.

Bluth, G.J.S., Watson, I.M., Rose, W.I., Realmuto, V.J, in prep. MODIS Retrievals of Volcanic Sulfur and Ash Emissions from Nyamuragira Volcano.

Carn, S.A., Krueger, A.J., Bluth, G.J.S., Schaefer, S.J., Krotkov, N.A., Watson, I.M., Datta, S., 2003. Volcanic eruption detection by the Total Ozone Mapping Spectrometer (TOMS) instrument: a 22 year record of sulfur dioxide and ash emissions. In: Oppenheimer, C., Pyle, D.M., Barclay, J. (Eds.), Volcanic Degassing. Geological Society London, Special Publication, 213, 177–203.

Casadevall, T.J., 1994. Volcanic ash and aviation safety. U.S. Geological Survey Bulletin 2047, 1–6.

Dean, K., Dehn, J., McNutt, S., Neal, C., Moore, R., Schneider, D., 2002. Satellite imagery proves essential for monitoring erupting Aleutian volcano. EOS, Transactions, AGU 83 (22), 241–247.

Krueger, A.J., Walter, L.S., Bhartia, P.K., Schnetzler, C.C., Krotkov, N.A., Sprod, I., Bluth, G.J.S., 1995. Volcanic sulfur dioxide measurements from the total ozone mapping spectrometer instruments. Journal of Geophysical Research 100 (D7), 14057–14076.

Lacis, A., Hansen, J., Sato, M., 1992. Climate forcing by stratospheric aerosols. Geophysical Research Letters 19, 1607–1610.

Oppenheimer, C., Francis, P., Stix, J., 1998. Depletion rates of SO_2 in tropospheric volcanic plumes. Geophysical Research Letters 25, 12249–12254.

Pollack, J.B., Toon, O.B., Khare, B.N., 1973. Optical properties of some terrestrial rocks and glasses. Icarus 19, 372–389.

Prata, A.J., 1989a. Infrared radiative transfer calculations for volcanic ash clouds. Geophysical Research Letters 16, 1293–1296.

Prata, A.J., 1989b. Observations of volcanic ash clouds in the 10–12 m window using AVHRR/2 data. International Journal of Remote Sensing 10, 751–761.

Prata, A.J., Bluth, G.J.S., Rose, W., Schneider, D., Tupper, A., 2001. Comments on 'Failures in detecting volcanic ash from a satellite-based technique'. Remote Sensing of Environment 78, 341–346.

Prata, A.J., Rose, W.I., Self, S., O'Brien, D., 2003. Global, long-term sulphur dioxide measurements from TOVS data: a new tool for studying explosive volcanism and climate. In: Robock, A., Oppenheimer, C. (Eds.), Volcanism and the Atmosphere. AGU Special Publication 139, 75–92.

Prata, A.J., Watson, I.M., Rose, W.I., Realmuto, V., Bluth, G.J.S., Sevranckx, R., in review. Volcanic sulfur dioxide measurements derived from infrared satellite measurements. Geophysical Research Letters.

Realmuto, V.J., 1990. Separating the effects of temperature and emissivity: emissivity spectrum normalization. In: Abbott, E.A. (Ed.), Proceedings of the 2nd TIMS workshop. JPL Publication 55–90, pp. 31–35.

Realmuto, V.J., 2001. The potential use of earth observing system data to monitor the passive emission of sulfur dioxide from volcanoes. Remote Sensing of Active Volcanism. In: Mouginis-Mark, P., Crisp, J., Fink, J. (Eds.), AGU Monograph 116, pp. 101–115.

Realmuto, V.J., Worden, H.M., 2000. The impact of atmospheric water vapor on the thermal infrared remote sensing of volcanic sulfur dioxide emissions: a case study from the Pu'u 'O'o vent of Kilauea Volcano, Hawaii. Journal of Geophysical Research 105, 21497–21508.

Realmuto, V.J., Watson, I.M, 2001. Advances in thermal infrared mapping of volcanic sulfur dioxide. EOS, Transactions, AGU 82 (47) (Fall. Meet. Suppl., Abstract V32F-09).

Realmuto, V.J., Abrams, M.J., Boungiorno, M.F., Pieri, D.C., 1994. The use of multispectral thermal infrared image data to estimate the sulfur dioxide flux from volcanoes: a case study from Mt. Etna, Sicily, 1994, July 29, 1986. Journal of Geophysical Research 99 (B1), 481–488.

Realmuto, V.J., Sutton, A.J., Elias, T., 1997. Multispectral thermal infrared mapping of sulfur dioxide plumes: a case study from the East Rift Zone of Kilauea Volcano, Hawaii. Journal of Geophysical Research 102 (B7), 15057–15072.

Rose, W.I., Delene, D.J., Schneider, D.J., Bluth, G.J.S., Krueger, A.J., Sprod, I., McKee, C., Davies, H.L., Ernst, G.G.J., 1995. Ice in Rabaul eruption cloud of 19–21 September 1994. Nature 375, 477–479.

Rose, W.I., Bluth, G.J.S., Ernst, G.G.J., 2000. Integrating retrievals of volcanic cloud characteristics from satellite remote sensors: a summary. Philosophical Transactions of the Royal Society of London 358, 1585–1606.

Rose, W.I., Bluth, G.J.S., Schneider, D.J., Ernst, G.G.J., Riley, C.M., McGimsey, R.G., 2001. Observations of 1992 Crater Peak/Spurr Volcanic Clouds in their first few days of atmospheric residence. Journal of Geology 109, 677–694.

Rose, W.I., Gu, Y., Watson, I.M., Yu, T., Bluth, G.J.S., Prata, A.J., Krueger, A.J., Krotkov, N., Carn, S., Fromm, M.D., Hunton, D.E., Ernst, G.G.J., Viggiano, A.A., Miller, T.M., Ballentin, J.O., Reeves, J.M., Wilson, J.C., Anderson, B.E., Flittner, D., in press. The February–March 2000 eruption of Hekla, Iceland from a satellite perspective. In: Robock, A., Oppenheimer, C., (Eds.), Volcanism and the Atmosphere. AGU Special Publication 39, 107–132.

Simpson, J.J., Hufford, G., Pieri, D., Berg, J., 2000. Failures in detecting volcanic ash from a satellite-based technique. Remote Sensing of Environment 72, 191–217.

Watson, I.M., Realmuto, V.J., Rose, W.I., Bluth, G.S.J., submitted for publication. Forward Modeling of Volcanic Cloud Transmissions Within Different Atmospheres. Journal of Geophysical Research-Atmospheres.

Watson, I.M., Realmuto, V.J., Rose, W.I., Bluth, G.S.J., Prata, A.J., Gu, Y., Rodriguez, L., in preparation. Observations of passive

degassing from Pacaya volcano using the Advanced Spaceborne Thermal Emission and Reflection Radiometer (ASTER), for Geophysical Research Letters.

Wen, S., Rose, W.I., 1994. Retrieval of sizes and total mass of particles in volcanic clouds using AVHRR bands 4 and 5. Journal of Geophysical Research-Atmospheres 99 (D3), 5421–5431.

Yu, T., Rose, W.I., 2001. Retrieval of Sulfate and Silicate Ash Masses in Young (1–4 Days Old) Eruption Clouds Using Multiband HIRS/2 Data. In: Mouginis-Mark, P., Crisp, J., Fink, J. (Eds.), Remote Sensing of Active Volcanism, pp. 87–100.

Yu, T., Rose, W.I., Prata, A.J., 2002. Atmospheric correction for satellite-based volcanic ash mapping and retrievals using "split window" IR data from GOES and AVHRR. Journal of Geophysical Research 106 (D16), 10.1029.